INL/EXT-11-23347

Reference Alloy Waste Form Fabrication and Initiation of Reducing Atmosphere and Reductive Additives Study on Alloy Waste Form Fabrication

S. M. Frank
T. P. O'Holleran
P. A. Hahn

September 2011

The INL is a U.S. Department of Energy National Laboratory
operated by Battelle Energy Alliance

INL/EXT-11-23347
FCR&D-WAST-2011-000089

Reference Alloy Waste Form Fabrication and Initiation of Reducing Atmosphere and Reductive Additives Study on Alloy Waste Form Fabrication

S. M. Frank
T. P. O'Holleran
P. A. Hahn

September 2011

Idaho National Laboratory
Fuel Cycle Research & Development
Idaho Falls, Idaho 83415

http://www.inl.gov

Prepared for the
U.S. Department of Energy
Office of Nuclear Energy
Under DOE Idaho Operations Office
Contract DE-AC07-05ID14517

SUMMARY

This report describes the fabrication of two reference alloy waste forms, RAW-1(Re) and RAW-(Tc) using an optimized loading and heating method. The composition of the alloy materials was based on a generalized formulation to process various proposed feed streams resulting from the processing of used fuel. Waste elements are introduced into molten steel during alloy fabrication and, upon solidification, become incorporated into durable iron-based intermetallic phases of the alloy waste form. The first alloy ingot contained surrogate (non-radioactive), transition-metal fission products with rhenium acting as a surrogate for technetium. The second alloy ingot contained the same components as the first ingot, but included radioactive Tc-99 instead of rhenium. Understanding technetium behavior in the waste form is of particular importance due the longevity of Tc-99 and its mobility in the biosphere in the oxide form. RAW-1(Re) and RAW-1(Tc) are currently being used as test specimens in the comprehensive testing program investigating the corrosion and radionuclide release mechanisms of the representative alloy waste form.

Also described in this report is the experimental plan to study the effects of reducing atmospheres and reducing additives to the alloy material during fabrication in an attempt to maximize the oxide content of waste streams that can be accommodated in the alloy waste form. Activities described in the experimental plan will be performed in FY12. The first aspect of the experimental plan is to study oxide formation on the alloy by introducing O_2 impurities in the melt cover gas or from added oxide impurities in the feed materials. Reducing atmospheres will then be introduced to the melt cover gas in an attempt to minimize oxide formation during alloy fabrication. The second phase of the experimental plan is to investigate melting parameters associated with alloy fabrication to allow the separation of slag and alloy components of the melt.

CONTENTS

FIGURES

TABLES

ACRONYMS

At%	atom percent
BSE	back scatter electron
CETE	Coupled End-To-End
EBR-II	Experimental Breeder Reactor-II
EDS	energy dispersive spectroscopy
FCR&D	Fuel Cycle Research & Development Program
MFC	Materials and Fuels Complex
MWF	Metal Waste Form
NIST	National Institute of Science and Technology
ppm	parts-per-million
RAW	reference alloy waste form
SEM	scanning electron microscopy
SRNL	Savannah River National Laboratory
UDS	undissolved solids
Wt%	weight percent
XRD	x-ray diffraction

Reference Alloy Waste Form Fabrication and Initiation of Reducing Atmosphere and Reductive Additives Study on Alloy Waste Form Fabrication

1. INTRODUCTION

Alloy materials have been developed to immobilize transition metal fission products collected during the electrochemical/pyrometallurgical treatment of used, metallic fuel [1]. It is plausible that the undissolved solids (UDS) and reduced Tc waste streams generated from aqueous treatment of used fuel could also be incorporated into alloy waste forms [2]. A generalized alloy formulation has been established to incorporate transition metal fission products from a range of possible waste streams [3]. Work in progress within the Alloy Waste Form Characterization FCR&D campaign is to optimize and fabricate small-scale alloy reference waste forms, perform characterization of the alloys, study the corrosion and radionuclide release behaviors of the alloy waste form, and to develop source term models that support performance assessment calculations for disposal options.

The objectives of the work presented in this report are to determine fabrication parameters and produce the small-scale reference alloy waste forms (RAWs) used for the characterization and testing phase of the project. The alloys were fabricated with both surrogate transition metal fission products and radioactive materials. Fabrication methods were based on previous experience in metal waste form production and on anticipated large-scale fabrication requirements. In addition, a study on the effects of reducing atmospheres and added reductants on waste form fabrication has been initiated this year and will continue into FY12.

The format of this report describes the fabrication of the surrogate alloys in which rhenium (Re) was used as a surrogate for technetium (Tc). Inspection of the first surrogate alloy produced indicated incomplete mixing and melting of the primary components. Loading of the base metal components into the crucible and an increase in the melt temperature produced a second surrogate alloy ingot with the desired alloy phase composition distributed homogeneously throughout the ingot. Once confidence in the small-scale fabrication method had been established a third ingot was produced that contained Tc instead of the surrogate Re. The hazardous nature of Tc-99, due to its very long half-life and mobility of Tc oxides in the biosphere, require that Tc be immobilized in a durable waste form. Technetium in the reduced or metallic state, such as found in the alloy waste form, is very stable and has very low release rates from the alloy [4]. Thus the alloy waste form is well suited for the immobilization of Tc.

This report completes the level 3 milestone requirement M31SW080205, Reducing Atmosphere and Reductive Additive Study on Alloy Waste Form Fabrication; and provides detail on level 3 milestone requirement M41SW0820, Fabrication of Reference Alloy waste Forms.

2. RAW-1(Re)

2.1 Fabrication of Raw-1(Re), 1600° C Melt

The initial RAW1-Re alloy was produced on December 8, 2010 with a composition shown in table 1. The suppliers for the various components were: stainless steel in chip form (SRM 160b) supplied by the National Institute of Standards and Technology, Gaithersburg, MD; Zr powder (-140 mesh, 99.8% pure) supplied by CERAC, Inc., Milwaukee, WI; Mo powder (-100 mesh, 99.95% pure) supplied by Alfa Aesar, Ward Hill, MA; Ru, Rh, Pd and Re supplied by ESPI Metals, Ashland, OR all with mesh sizes of -325 and purities of 99.95% with the exception of Rh with a mesh size of -60.

Table 1. Composition of RAW-1(Re), 1600° C melt.

	Stainless Steel	Zr	Mo	Ru	Rh	Pd	Re
Mass Added (g)	29.335	6.061	5.528	3.746	0.682	2.508	2.428
Weight % in ingot	58.33	12.05	12.31*	2.49	7.44	4.99	4.83

*1.32 wt% Mo contributed from stainless steel

The metal components were loaded in to a 20 cm^3 yttria (Y_3O_2) crucible (Hadron Technologies, Arvada, CO) using the following formulation: a layer of stainless steel chips were first added to the bottom of the crucible followed by addition of the Zr, Mo, Ru, Rh Pd and Re powders that had previously been mixed together in a polyethylene bottle, and lastly addition of the remaining stainless steel to the top of the powder. All material handling and fabrication was performed under an Ar atmosphere. After crucible loading, an yttria cap was placed on top of the crucible and the loaded crucible then placed in a larger zirconia crucible to act as containment for the metal loaded crucible. The crucibles were then placed into a high-temperature resistive furnace (CM Furnace, model 1704 furnace with Kanthal™ 1800 molydisilicide heating elements and a 4”x4”x4” heating zone, Bloomfield, N.J.) The furnace had been modified and placed inside an Ar atmosphere, radiological glovebox with the controller external to the glovebox. The glovebox atmosphere was maintained with oxygen and moisture contamination typically below 20 ppm. Images of the loaded crucible and the crucibles in the furnace are shown in figure 1.

The purpose of adding the majority of the lower melting point stainless steel to the top of the mixture was to wet the high melting point components and form lower melting eutectic phases. To accomplish this, the furnace was heated to 1600° C with a ramp rate of 20° C/min and held for approximately 1 hour as shown in the heating profile of figure 2. After holding at the maximum temperature, the furnace was allowed to cool to 1100° C (ramped down at 10° C/min) and held for another hour. This 1100° C hold was essentially an anneal step to allow the ingrowth of favorable intermetallic phases.

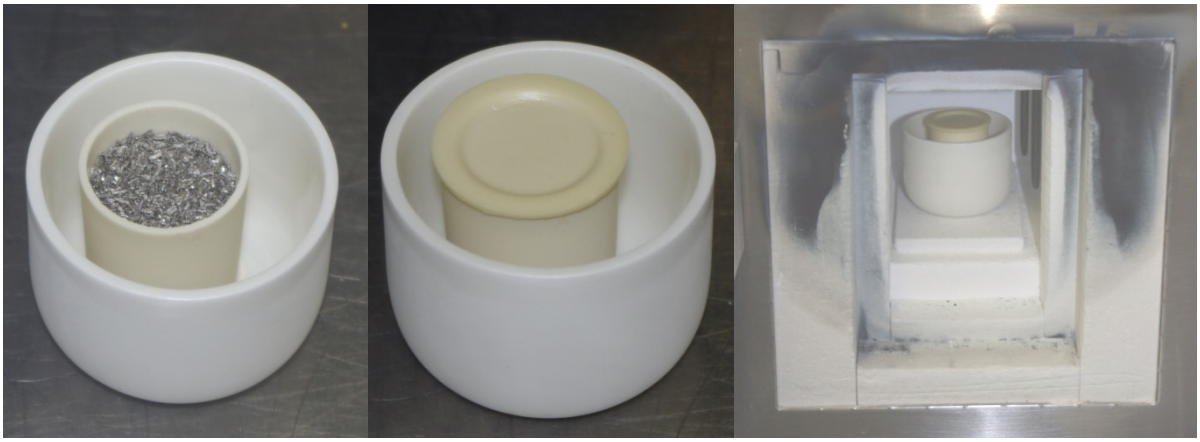

Figure 1. Left-hand image, loaded yttria crucible inside zirconia crucible. Middle image, yttria crucible with cap. Right-hand image, nested crucibles inside furnace heat zone.

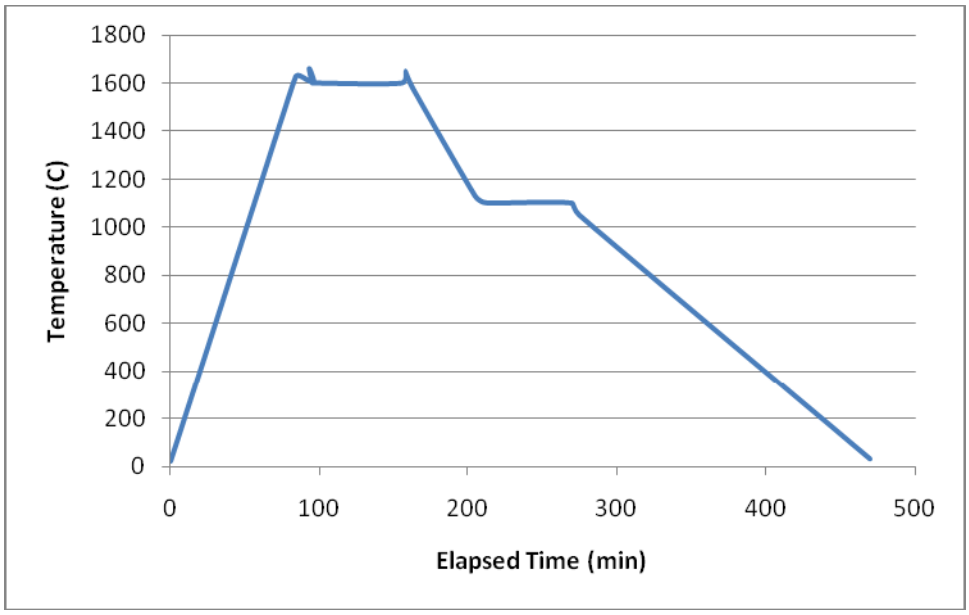

Figure 2. 1600° C heating profile for RAW-1(Re), first melt alloy with anneal step at 1100° C.

Observation of the RAW-1(Re) alloy from the first melt indicated that there was possibly incomplete mixing. A large metallic sphere was also observed attached to the bottom of the concaved shaped ingot as shown in the figure 3. Furthermore, small metallic spheres and a larger metallic flake material were observed adhering to the crucible walls, the cap and the bottom of the crucible as shown in figure 4. The dark metallic flake material adhered to the bottom of the crucible weighted 0.5068 g and had a composition similar to stainless steel as determined by XRD and SEM. There was also a fine yellowish deposit on the bottom of the crucible similar in color to the bottom of the ingot. The mass of the initial charge was 50.242 g and the final ingot weight was 49.665 g. With the added mass of the flaky deposit on the bottom of the crucible, the recovered mass was 50.172 g.

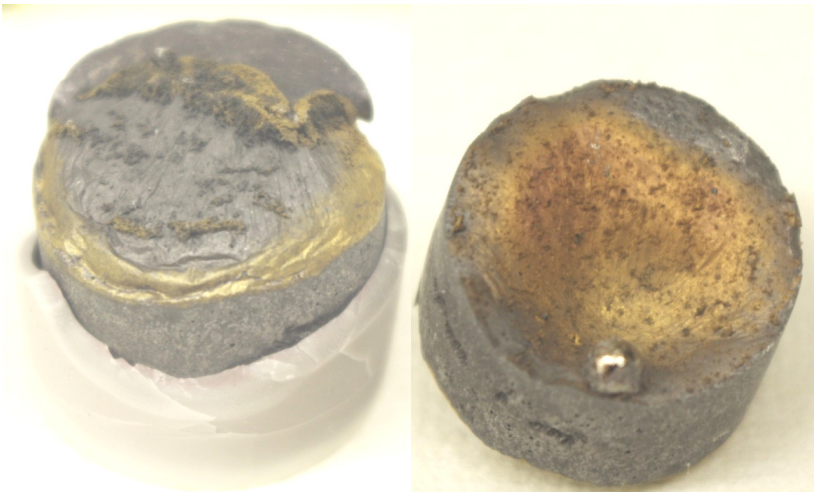

Figure 3. Left-hand image, RAW-1(Re) ingot from 1600° C in broken yttria crucible and the bottom of the ingot (right-hand image) with the attached metallic sphere and gold colored surface layer.

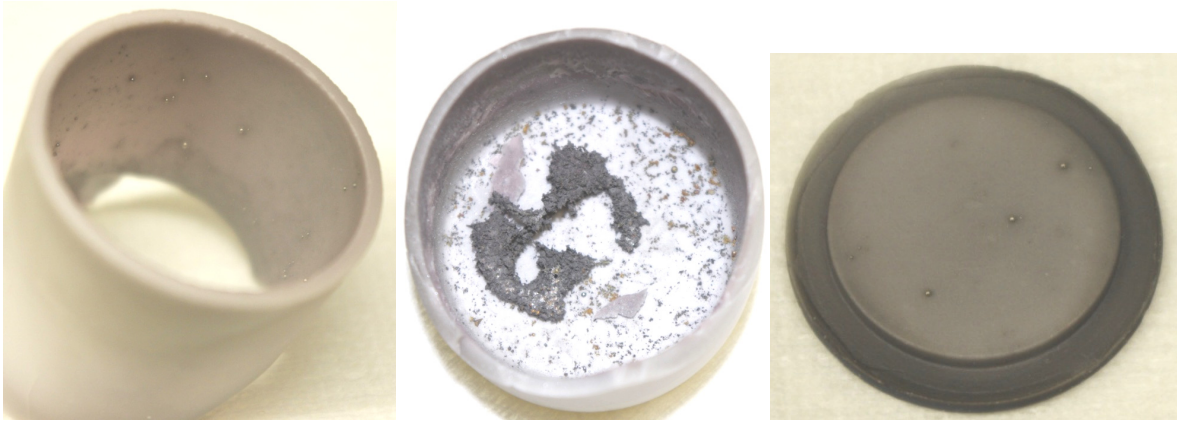

Figure 4. Metallic deposits on crucible surfaces after first RAW-1(Re) melt.

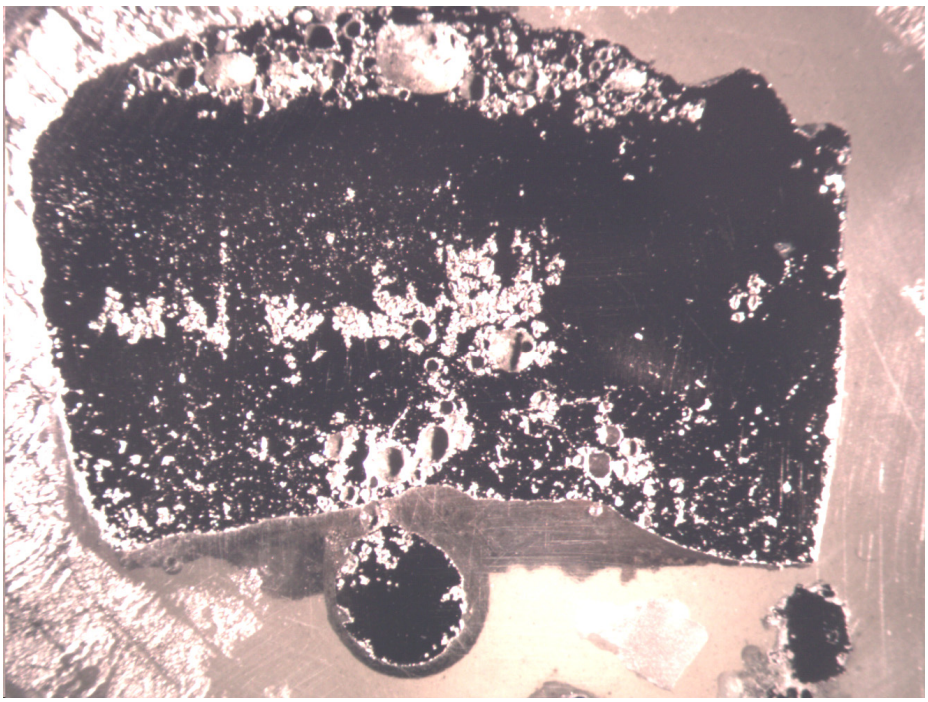

Figure 5. Optical image of the RAW-1(Re) 1600° C melt, mounted cross-section used for microscopy analysis. The image shows non-consolidated, open void regions on top and bottom of the ingot and the attached metallic sphere on the bottom of the ingot.

2.1.1 Electron Microscopy Analysis of RAW-1(Re), 1600° C Melt

Scanning electron microscopy (SEM) analysis of the sample was performed using a LEO 1455UP SEM (Carl Zeiss, LLC North America) with an Oxford Instruments, INCAx Systems x-ray energy dispersive spectrometer (EDS) detector (Oxfordshire, UK) used for elemental analysis. Samples were mounted in epoxy and polished to a 1200 grit finish and then coated with carbon to prevent beam charging. Figure 6 shows backscattered electron (BSE) images from the top, middle and bottom regions of the cut ingot. While the top region shows what appears to be intermetallic and solid solution phases, these phase regions appear to be less developed toward the bottom of the ingot. Table 2 shows the elemental composition of various regions of the ingot as determined by EDS. When this data was compiled, Fe was not included in the total composition, so element concentrations are normalized to higher concentrations than are actually present in the sample. The elemental composition shows some non-homogeneity between different regions of the ingot as suspected from visual inspection.

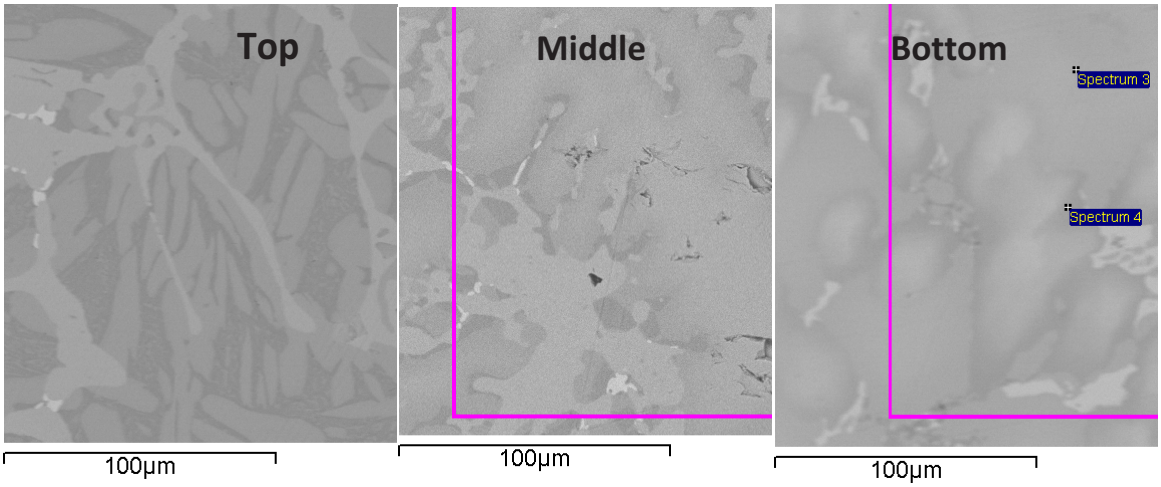

Figure 6. Backscattered electron images of the RAW-1(Re) from the 1600° C melt showing the surface morphology from the top to the bottom of the ingot with less well defined phase regions at the bottom of the ingot.

Table 2. Elemental composition from various regions of the RAW-1(Re) ingot, 1600° C Melt.

Location	Mean Elemental Composition (Weight %)									
	Cr	Mn	Fe	Ni	Zr	Mo	Ru	Rh	Pd	Re
Top Slag	30	2.6	NM	19	15	13	7.9	1.8	8.0	3.1
Top	32	2.8	NM	16	12.6	16	8.8	0.93	5.9	5.0
Middle	20	1.7	NM	15	16	12	8.7	2.2	20	5.2
Bottom	11	0.94	NM	7.8	19	17	14	3.4	21	5.2
Round Inclusion	13	1.7	NM	9.7	20	14	14	3.2	23	1.2
Metallic Flake	44	2.9	NM	28	13	9.1	0.69	0.0	1.1	1.1
Target	11	0.95	38	7.2	12	12	7.4	1.3	5.0	4.6

NM – not measured

Based on visual, microscopy imaging and EDS element determination from different regions of the ingot, it was determined that the ingot was not sufficiently consolidated nor had a uniform phase distribution formed within the ingot. It appeared that insufficient melting had occurred during the first melt and that the higher melting temperature components (Zr, Mo, Ru, Rh, Pd and Re) were not adequately wetted by the stainless steel to form lower melting eutectic phases. It was then decided to fabricate a second surrogate RAW-1(Re) ingot by altering the method for crucible loading with the base components (mixing some of the stainless steel in with the metal powders) and to vary the heating profile to a slightly higher melting temperature of 1650° C.

2.2 Fabrication of RAW-1(Re), 1650° C Melt

The second RAW-1(Re) ingot was produced on January 5, 2011 in a similar manner to the first ingot by using the same materials handled under an inert Ar atmosphere, but with modifications to the crucible loading method and by increasing the melt temperature to 1650° C (max temp 1674° C due to furnace overtemp for ~10 minutes). The crucible loading for the second RAW-1(Re) ingot involved adding 10.06 g (~ 34 wt%) of the stainless steel to the powder components (Mo, Zr, Ru, Rh, Pd, and Re) and premixing before adding to the crucible. Initially, 4.4 g of stainless steel was added to the bottom of the crucible, the metal powder/stainless steel mixture was then added to the crucible, and finally the remainder of the stainless steel (14.81 g or 50%) was added to the top of the charge to completely cover the powder mixture. Table 3 provides the elemental composition of the second RAW-1(Re) alloy, and figure 7 shows the 1650° C heat profile.

Table 3. Composition of RAW-1(Re), 1650° C Melt.

	Stainless Steel	Zr	Mo	Ru	Rh	Pd	Re
Mass Added (g)	29.29	5.98	5.50	3.80	0.60	2.56	2.20
Weight % in ingot	58.7	12.0	12.3*	7.6	1.2	5.1	4.4

*1.32 wt% Mo contributed from stainless steel

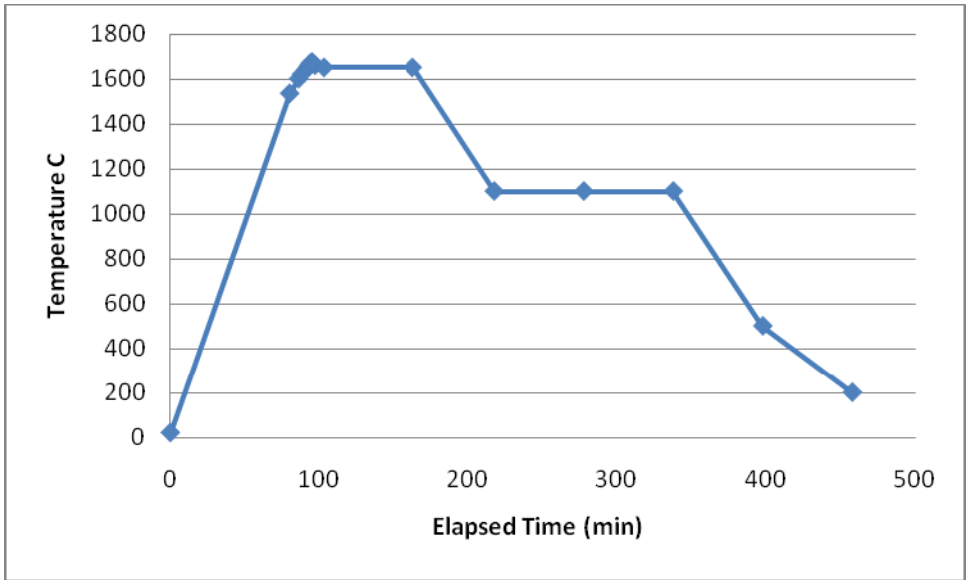

Figure 7. 1650° C heating profile used to fabricate the second RAW-1(Re) alloy ingot. Actual maximum temperature was 1674° C for approximately 10 minutes due to furnace overtemp.

The second RAW-1(Re) ingot produced at 1650° C looked superior to the first ingot produced at the lower temperature of 1600° C. No deposit or separate phases were observed on the ingot

or crucible except the slight deposit on the bottom of the crucible as shown in figure 8. The ingot itself was well formed with no concavity on the bottom and with a gold surface layer on the surface similar to the first ingot and this material was later identified as zirconium oxide [5]. A cut section from one side of the ingot was obtained using a slow speed saw with abrasive blade (Buelher IsoMet® saw, Lake Bluff, IL), and the cut section prepared for microscopy as described earlier.

Figure 8. Second RAW-1(Re) ingot fabricated at 1650° C. Left-hand image, ingot and broken bottom crucible. Middle image, top of ingot showing gold colored zirconium oxide surface layer. Right-hand image, bottom of ingot with on visible surface layers.

2.2.1 Electron Microscopy Analysis of RAW-1(Re), 1650° C Melt

Large-area (~680 µm x 511 µm) micrograph images and x-ray elemental analysis was performed on three areas from the top, middle and bottom regions of the sectioned RAW-1(Re) ingot. Analysis of the three areas analyzed across the top, middle and bottom of the ingot concluded that the elemental composition and phase distribution was indistinguishable between the different regions of the ingot. Figure 9 shows the BSE image from the three areas of the top, middle and bottom regions of the ingot. Table 4 provides the x-ray EDS elemental composition for the same areas in the micrographs. Table 5 provides the overall average elemental composition of RAW-1(Re) prepared from the second melt.

Modifications to the crucible loading method and the increase of melt temperature resulted in the formation of a well compacted alloy ingot that was homogeneous with respect to elemental composition and phase distribution throughout the ingot at the spatial resolution of the electron microscopy analysis. With favorable results obtained after modification to the crucible loading procedure and increased melt temperature, it was decided to proceed with the fabrication of the 50 g RAW ingot containing Tc.

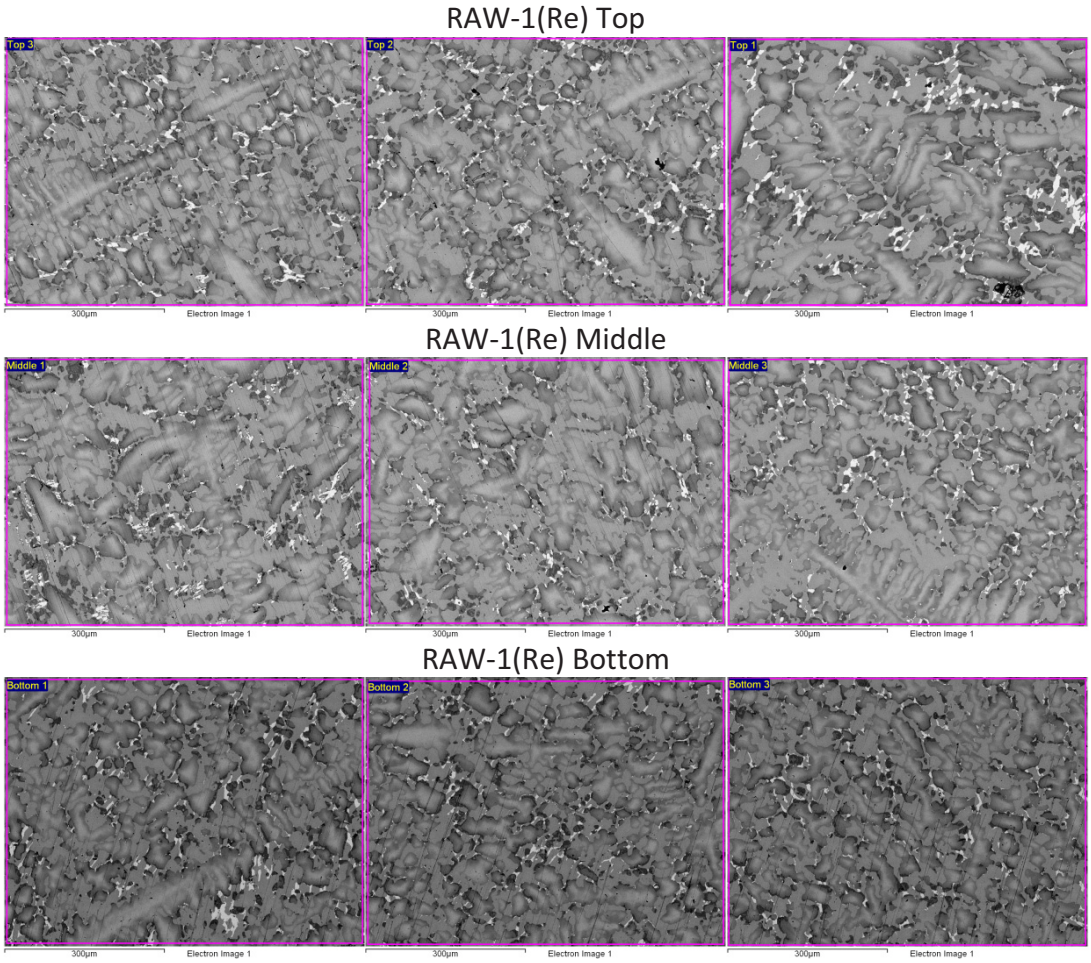

Figure 9. Electron micrographs of RAW-1(Re) alloy ingot prepared at 1650° C. The images compare the microstructure and phase distribution of three areas from the top, middle and bottom of the sectioned ingot. No significant difference in phase distribution is observed from different regions of the ingot.

Table 4. Elemental composition from three areas from the top, middle and bottom regions of the RAW-1(Re) ingot produced at 1650° C. Concentrations are given in both weight% and atomic%.

	Top 1		Top 2		Top 3		Top Ave			
	Wt%	At%	Wt%	At%	Wt%	At%	Wt%	Wt% STD	At%	At% STD
Cr	10.09	13.69	10.79	14.51	10.67	14.40	10.52	0.37	14.20	0.45
Mn	1.05	1.35	1.02	1.30	1.06	1.35	1.04	0.02	1.33	0.03
Fe	34.64	43.77	35.41	44.32	35.11	44.12	35.05	0.39	44.07	0.28
Ni	6.95	8.36	6.91	8.23	6.85	8.18	6.90	0.05	8.26	0.09
Zr	13.46	10.41	13.23	10.14	13.46	10.35	13.38	0.13	10.30	0.14
Mo	12.93	9.51	13.55	9.87	13.18	9.64	13.22	0.31	9.67	0.18
Ru	8.26	5.77	7.92	5.48	8.21	5.70	8.13	0.18	5.65	0.15
Rh	1.29	0.89	1.10	0.75	1.22	0.83	1.20	0.10	0.82	0.07
Pd	6.90	4.57	5.77	3.79	5.57	3.67	6.08	0.72	4.01	0.49
Re	4.42	1.68	4.30	1.61	4.69	1.77	4.47	0.20	1.69	0.08
	Middle 1		Middle 2		Middle 3		Middle Ave			
	Wt%	At%	Wt%	At%	Wt%	At%	Wt%	Wt% STD	At%	At% STD
Cr	9.99	13.56	10.70	14.44	10.33	13.92	10.34	0.36	13.97	0.44
Mn	1.01	1.29	1.08	1.38	1.13	1.44	1.07	0.06	1.37	0.08
Fe	34.40	43.46	35.01	43.99	35.32	44.32	34.91	0.47	43.92	0.43
Ni	7.01	8.43	6.92	8.27	7.18	8.58	7.04	0.13	8.43	0.16
Zr	14.79	11.44	12.92	9.94	13.26	10.19	13.66	1.00	10.52	0.80
Mo	12.97	9.54	14.35	10.50	13.39	9.78	13.57	0.71	9.94	0.50
Ru	8.28	5.78	8.03	5.57	8.05	5.58	8.12	0.14	5.64	0.12
Rh	1.25	0.86	1.13	0.77	1.03	0.70	1.14	0.11	0.78	0.08
Pd	6.14	4.07	5.03	3.32	5.68	3.74	5.62	0.56	3.71	0.38
Re	4.17	1.58	4.83	1.82	4.63	1.74	4.54	0.34	1.71	0.12
	Bottom 1		Bottom 2		Bottom 3		Bottom Ave			
	Wt%	At%	Wt%	At%	Wt%	At%	Wt%	Wt% STD	At%	At% STD
Cr	10.65	14.35	10.89	14.63	10.49	14.11	10.68	0.20	14.36	0.26
Mn	1.00	1.27	1.02	1.30	0.93	1.18	0.98	0.05	1.25	0.06
Fe	35.18	44.15	35.73	44.70	35.55	44.50	35.49	0.28	44.45	0.28
Ni	7.25	8.66	7.00	8.33	7.19	8.57	7.15	0.13	8.52	0.17
Zr	12.95	9.95	12.34	9.45	13.06	10.01	12.78	0.39	9.80	0.31
Mo	13.23	9.66	13.51	9.84	13.43	9.79	13.39	0.14	9.76	0.09
Ru	7.89	5.47	8.06	5.57	8.19	5.66	8.05	0.15	5.57	0.10
Rh	1.18	0.81	1.33	0.90	1.41	0.96	1.31	0.12	0.89	0.08
Pd	5.88	3.87	5.25	3.45	5.53	3.64	5.55	0.32	3.65	0.21
Re	4.79	1.80	4.86	1.82	4.22	1.59	4.62	0.35	1.74	0.13

Table 5. Overall average elemental composition of RAW-1(Re) ingot prepared at 1650° C.

Average Composition (Ave of Top, Middle, Bottom)				
	Wt%	Std	At%	Std
Cr	10.51	0.17	14.18	0.20
Mn	1.03	0.05	1.32	0.06
Fe	35.15	0.30	44.15	0.27
Ni	7.03	0.12	8.40	0.13
Zr	13.27	0.45	10.21	0.37
Mo	13.39	0.18	9.79	0.14
Ru	8.10	0.05	5.62	0.05
Rh	1.22	0.09	0.83	0.06
Pd	5.75	0.29	3.79	0.19
Re	4.55	0.08	1.71	0.03

3. RAW-1(Tc)

3.1 Fabrication of RAW-1(Tc)

The 50.12 g RAW-1 (Tc) charge was blended on January 21, 2011 with a composition shown in table 6. The method and materials used to produce the RAW-1(Tc) ingot was the same used for second RAW-1(Re) ingot prepared at 1650° C. The exception to the fabrication method was the substitution of Tc for surrogate Re in the alloy waste form. The Tc was obtained from Oak Ridge National Laboratory, Oak Ridge TN, as ammonium pertectnetate in fine powder form. This material was then reduced to the elemental state under a H_2/Ar mixture at 940° C. The purity of the Tc metal was determined to be 97.3 ± 5 wt%.

Table 6. Composition of 50 g RAW-1(Tc) alloy ingot.

	Stainless Steel	Zr	Mo	Tc	Ru	Rh	Pd
Mass Added (g)	30.08	6.14	5.60	1.25	3.81	0.67	2.57
Weight % in ingot	60.02	12.35	12.49*	2.49	7.60	1.34	5.13

*1.37 wt% Mo contributed from stainless steel

As mentioned earlier, loading of the crucible involved mixing the Zr, Mo, Tc, Ru, Rh and Pd powders together with 10 g of the stainless steel chips. Approximately 4 g of the stainless steel chips were added to the bottom of a 20 cm^3 yttria crucible followed by addition of the metal powder/stainless steel mixture to the crucible. Lastly, the remainder of the stainless steel (~16 g) was added to the crucible as shown in figure 10. All material handling and fabrication was performed under an Ar atmosphere with oxygen and moisture contamination below 20 ppm. A

nine week delay followed crucible loading and heating of the material to form the reference alloy due to a radiological work stand down. The material remained under an Ar atmosphere during that time in a closed container.

Figure 10. Left-hand image, loaded yttria crucible with top layer of stainless steel chips. Right-hand image, loaded yttria crucible with cap placed inside zirconia crucible prior to heating.

Constituent mixing and the heating profile had previous been optimized during fabrication of the RAW-1(Re) surrogate alloy. The optimized heating profile is shown in figure 7 with a maximum temperature of 1675° C obtained before the furnace stabilized at 1650° C. During the heating of the RAW-1(Tc) alloy however, one of the furnace controlling thermal couples failed during the heat cycle and had to be replaced. The actual heat profile during the fabrication of RAW-1(Tc) is shown in figure 11.

Figure 12 shows the crucible and ingot after fabrication, while figure 13 shows enlarged views of the top and bottom of the RAW-1(Tc) ingot. After fabrication, a section of the ingot was obtained from one side and mounted for scanning electron microscopy (SEM) analysis. The remainder of the ingot was sent to ANL for additional sampling, characterization and testing.

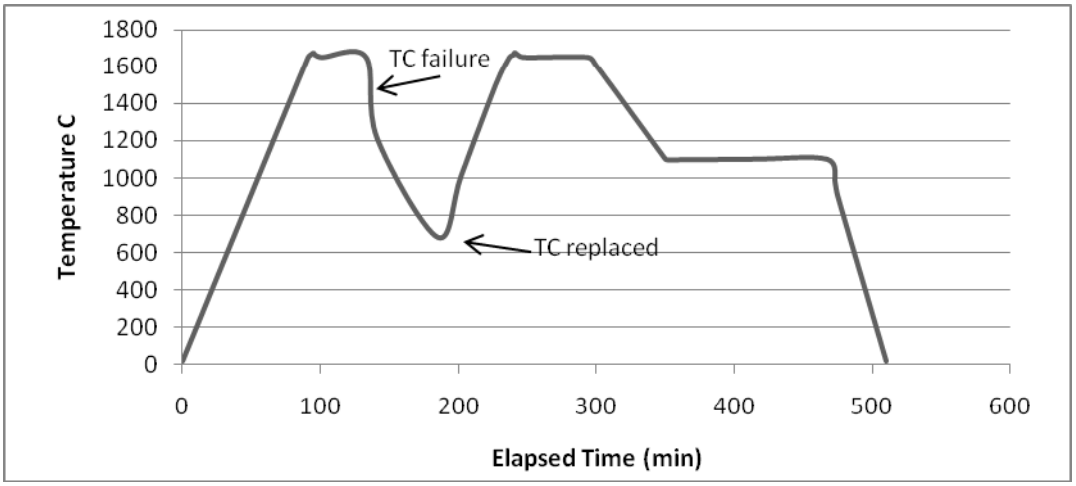

Figure 11. Top, optimized RAW-1 alloy heat profile. Bottom, RAW-1(Tc) heat profile showing thermal couple (TC) failure and replacement during alloy fabrication. The optimized heat profile reaches a maximum furnace temperature of 1675° C before stabilizing to 1650° C for 90 minutes before cool down.

Figure 12. Left-hand image shows the RAW-1(Tc) ingot in the yttria crucible after fabrication. Also shown is the crucible cap and the larger zirconia crucible that contained the yttria crucible during heating. The right-hand image shows the RAW-1(Tc) ingot after removal from the yttria crucible. A minimal amount of material remained in the yttria crucible.

Figure 13. Left-hand image shows the top of RAW-1(Tc). The gold colored surface feature is a thin layer or "slag" layer of zirconium oxide. It is unknown if the zirconium oxide surface layer forms from oxide contaminates found in the base constituents, or if the layer forms from reaction with oxygen contamination in the crucibles and glovebox Ar atmosphere during fabrication. The right-hand image shows the bottom to the ingot with no visible indication of a zirconium oxide slag layer.

3.1.1 Electron Microscopy Analysis of RAW-1(Tc)

The cut sample from the RAW-1(Tc) ingot was polished to 1200 grit, mounted in an epoxy holder and coated with a layer of carbon to prevent charging from the electron beam. The microstructure of the sample was very similar from top to bottom of the cut sample as illustrated in figure 14. The morphology of the RAW-1(Tc) sample was also very similar to the surrogate alloy RAW-1(Re). The elemental composition is presented in table 7 and appears homogeneous over the areas analyzed.

Figure 15 compares the microstructure morphologies between RAW-1 (Tc) and the surrogate alloy RAW-1(Re). The microstructure of the two alloys is very similar showing four different contrast and elemental composition phases of dendritic structure. In addition the phase composition of the two alloys is identical, with the exception of Tc substituting for Re, as shown in the higher magnification image of figure 16. Figure 17 shows the elemental x-ray color maps for major elements obtained from the area shown in figure 16, while table 8 provides the tabulated elemental composition values for the four distinct phase identified in figure 7 (white, light-gray, gray and dark-gray contrast phases).

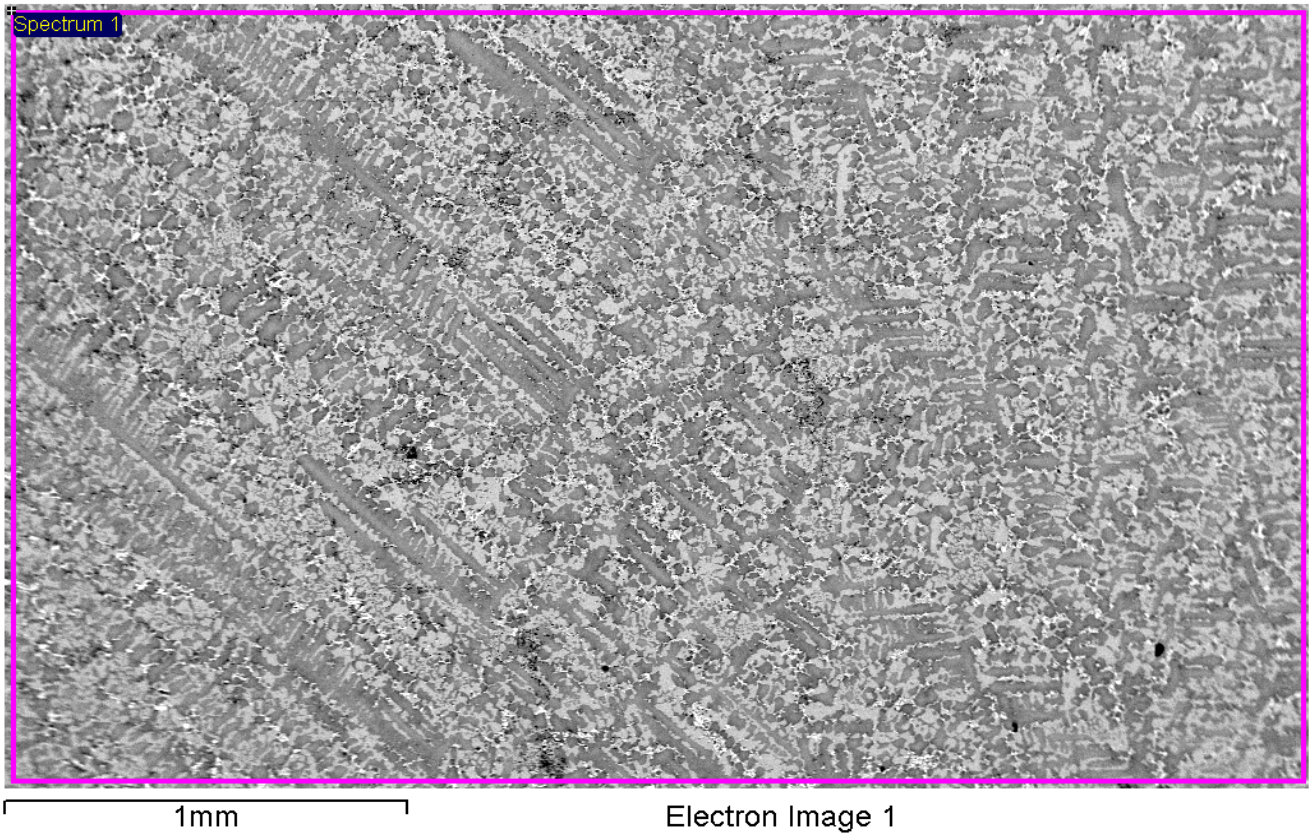

Figure 14. BSE image of center region of cut section from RAW-1(Tc).

Table 7. Large-area elemental composition of RAW-1(Tc) obtained from figure 5.

Composition	Element									
	Cr	Mn	Fe	Ni	Zr	Mo	Tc	Ru	Rh	Pd
Weight %	11.0	1.0	37.1	7.1	12.1	13.3	3.3	7.7	2.0	5.6
Atom %	14.4	1.2	45.4	8.2	9.0	9.4	2.3	5.2	1.3	3.6

With the completion of the preliminary RAW-1(Tc) microscopic analysis, the alloy ingot was deemed suitable for further testing and characterization. RAW-1(Tc) was then sent to Argonne National Laboratory on June 13, 2011 for further sampling and distribution to partner laboratories to begin more in-depth testing.

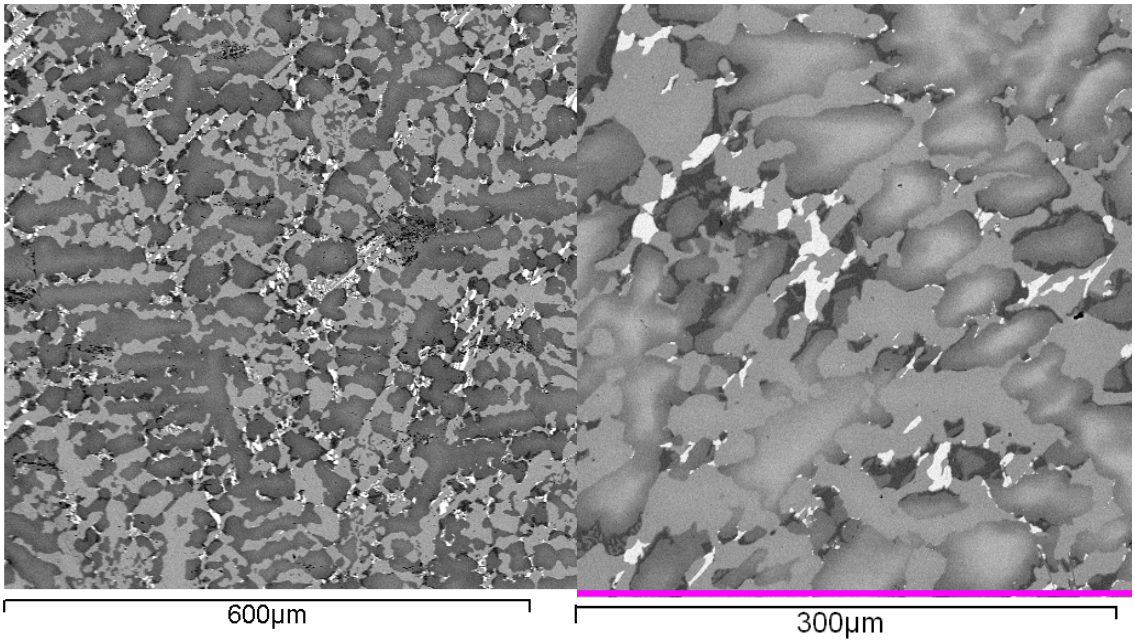

Figure 15. Backscatter electron micrograph comparison of RAW-1(Tc) (left-hand image) and RAW-1(Re) (right-hand image) showing similar microstructure morphologies. Note the difference in magnification between the two images.

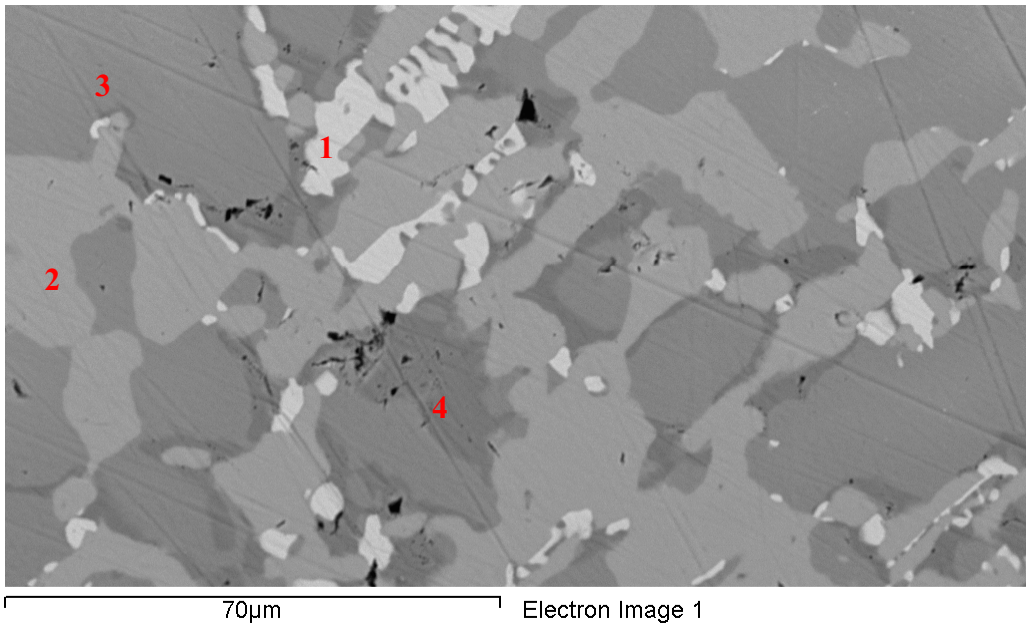

Figure 16. Higher magnification, backscatter electron image of RAW-1(Tc) with the four distinct phase compositions indicated (1, white phase; 2, light-gray phase; 3 gray phase; and 4, dark-gray phase).

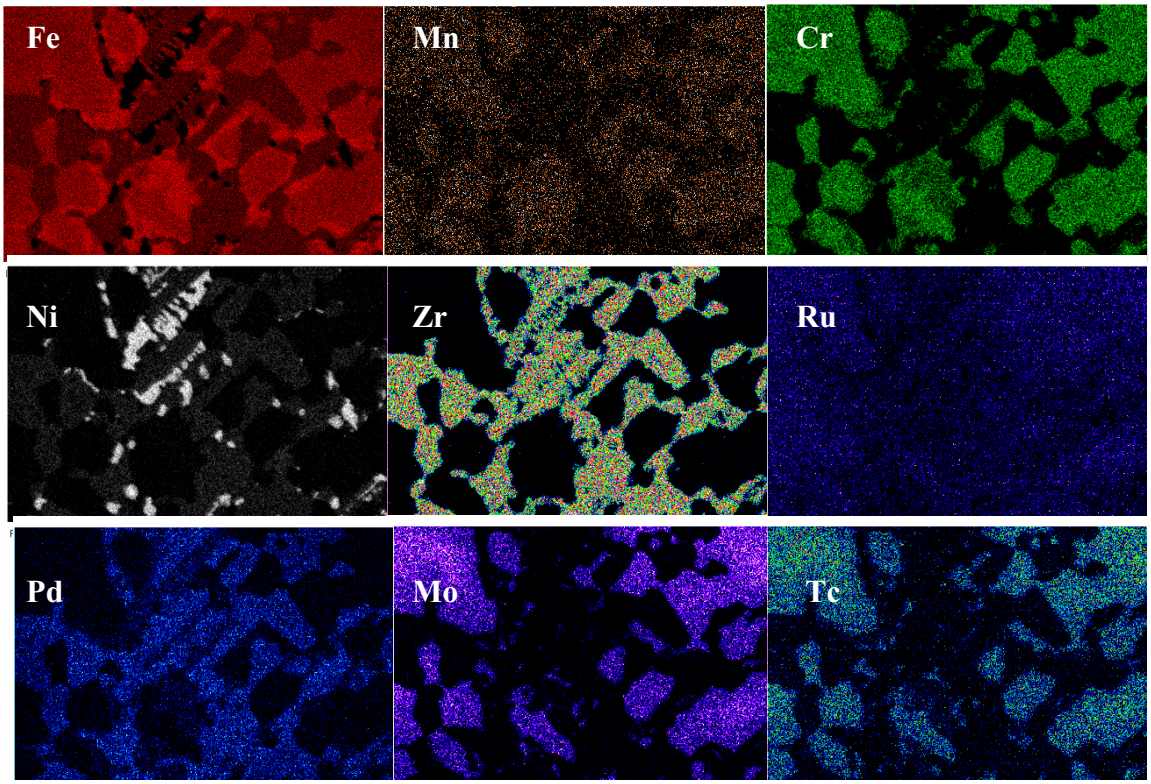

Figure 17. Elemental, color x-ray maps for area shown in figure 16.

Table 8. Elemental composition in atom % of the four distinct contrast phases identified in figure 16.

Phase	Average Element Composition (Atomic %) ± std dev									
	Cr	Mn	Fe	Ni	Zr	Mo	Tc	Ru	Rh	Pd
white (1)	ND	ND	3.3 ± 0.5	12.4 ± 0.3	23.6 ± 0.2	ND	ND	1.4 ± 0.5	5.0 ± 0.4	54.0 ± 0.4
light-gray (2)	4.3 ± 0.6	1.3 ± 0.2	37.1 ± 0.8	16.1 ± 1.4	22.8 ± 0.7	3.2 ± 0.8	1.1 ± 0.1	7.1 ± 0.5	1.9 ± 0.1	5.7 ± 0.9
gray (3)	21.0 ± 0.3	1.3 ± 0.2	49.9 ± 2.9	4.2 ± 0.4	ND	14.8 ± 1.6	3.3 ± 0.8	4.7 ± 0.3	ND	ND
dark-gray (4)	14.6 ± 0.3	1.7 ± 0.2	66.4 ± 0.8	8.9 ± 0.4	ND	3.7 ± 0.3	1.2 ± 0.2	3.3 ± 0.3	ND	ND

ND – not detected

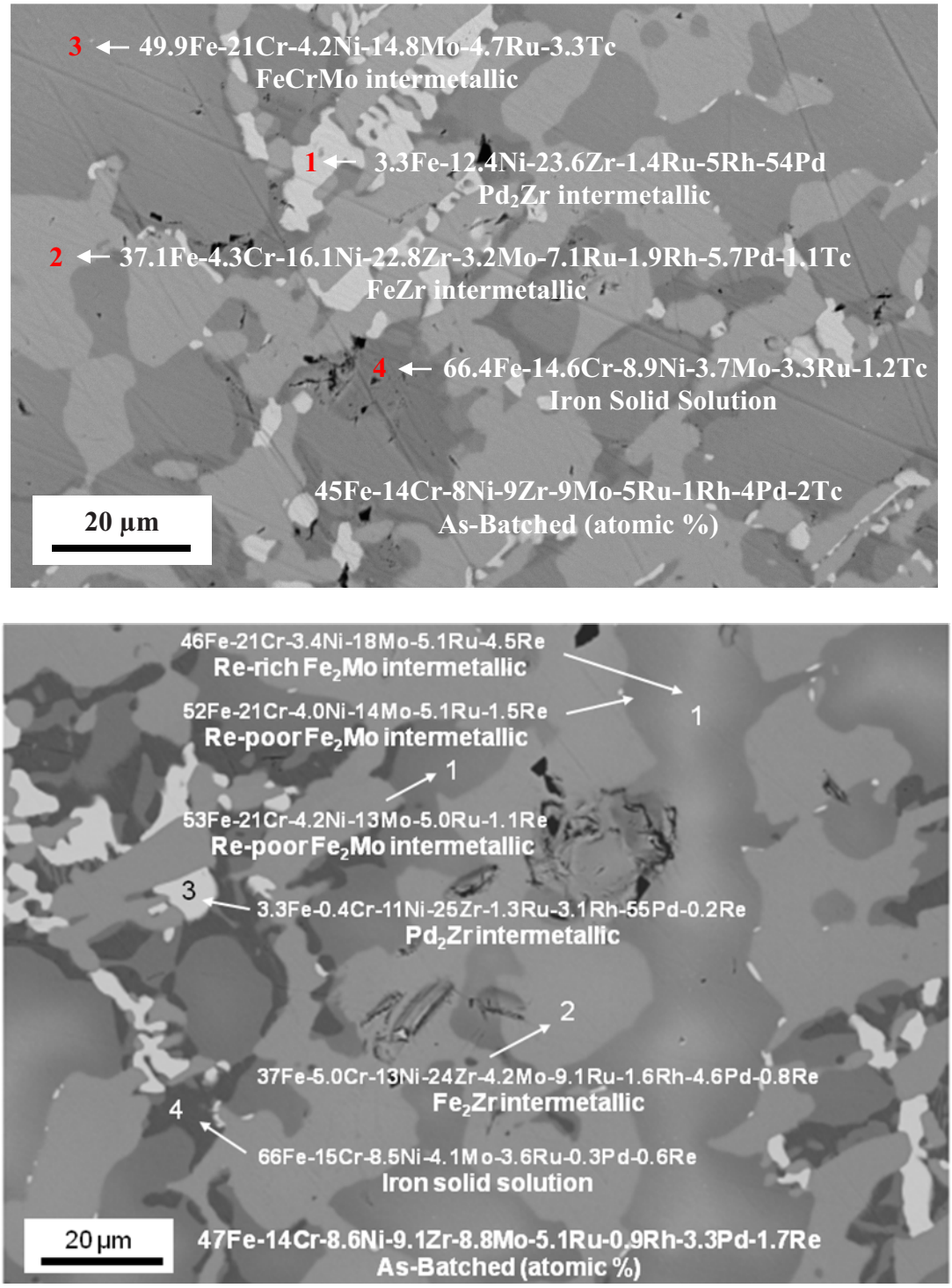

Figure 18. Comparison of phase composition from RAW-1(Tc) (top image) and RAW-2(Re) (bottom image). Both alloys show similar phase compositions for the Fe_2Mo, Fe_2Zr, Pd_2Zr, intermetallic phases and the Fe solid solution phase. Tc-rich and Tc-poor Fe_2Mo intermetallic phases were not identified during the preliminary microstructure analysis of the RAW-1(Tc) alloy.

4. Initiation of Reducing Atmosphere and Reductive Additives Study on Alloy Waste Form Fabrication

The RAW-1 alloys were made with metallic reagents to study the degradation behaviors of the intermetallic and iron solid solution phases that form. Actual waste streams from aqueous reprocessing operations will include large amounts of oxides. It is expected that some oxides could be reduced to metals prior to processing the waste streams to form an alloy waste form, but other oxides could not be reduced, particularly ZrO_2, which is expected to be abundant in aqueous processing waste streams. ZrO_2 itself is durable and its presence as a separate slag phase would be acceptable. A study was initiated to determine if reducing conditions during alloy fabrication could be used to reduce oxides in the waste form during the processing operation. This would allow an increase the amount of oxide-bearing wastes that can be incorporated in to the alloy. Two approaches can be applied to increase the reducing conditions during alloy fabrication; one approach is to increase the reducing nature of the atmosphere over the melt, and another is to add a solid reductant to the base components before melting with the end result the same for both approaches – that is to reduce the oxides to the metallic state which is more suitable for incorporation into the alloy waste form.

Oxide content in the alloy waste form could greatly affect the fabrication process, the physical and chemical integrity, or the performance of the final waste form. Unfortunately, oxide contents in the waste streams and the effects to the alloy are not well established at this time. For this study, two initial oxide conditions to alloy fabrication will be investigated. The first is oxide formation during fabrication due to oxygen impurities in the base components of the alloy or in the furnace environment. The second condition would be significant oxide content of approximately 10 weight percent or greater, in the feed stream. This investigation will deal only with these two scenarios as described in the following sections.

4.1 Effect of Reducing Atmosphere on Oxide Formation in the Alloy Waste Form

Based on metal waste form (MWF) development and production during the treatment of Experimental Breeder Reactor–II (EBR-II) fuel [6], oxide formation in the MWF from oxygen or moisture impurities, originating as impurities in the base components or from impurities in facility or furnace atmosphere, has never been identified as a significant problem for waste form fabrication or waste form performance as long as the impurities are kept relatively low in the system. Relatively low oxygen or moisture impurities in this context would be 500 ppm or less in the atmosphere above the melt, or less than 1 wt% in the feed stream. These limits are somewhat arbitrary, but are based on typical operating conditions found in the MWF processing facility and on observations found during the MWF development program.

What was observed during the MWF development program and during current MWF production is the formation of a thin-surface slag layer on the top of the ingot [7]. This slag

layer consists primarily of metal oxides, but other components could be present such as metal carbides. The exact source of the impurities is assumed to come from a combination of processing facility atmosphere impurities, impurities introduced from processing equipment such as crucibles and furnaces, and impurities found in the feed components used to make the MWF.

Initial investigation of the MWF slag layer found that the oxide layer is well bound to the underlying metal and is very durable, essentially providing a passivating layer to the metal surface of the waste form ingot [7]. From these observations and due to more pressing concerns regarding the development and implementation of MWF production, it was concluded that the slag layer formation of the MWF ingots produced from a pyrometallurgical process was not a concern to the fabrication and performance of the waste form, as long as impurities were kept as low as reasonably achievable. Furthermore, the slag might actually increase the durability of the material.

For this study however, where greater levels of oxide impurities are expected due to the nature of the waste stream feed, it is desirable to investigate methods to minimize oxide formation to the alloy waste form. To achieve this goal an experimental plan has been developed to study oxide formation on alloy ingots and to investigate methods to minimize the formation by controlling the reducing nature of the inert atmosphere over the melt during alloy fabrication. Several experimental methods are possible. One method is to introduce controlled atmospheres to the actual high-temperature furnace, located in the Ar atmosphere glovebox, currently used to make the RAW ingots at MFC, however; this method was discarded due to the large volume of gases required to produce the desired atmospheric mixture inside the glovebox, and the possibility of potential damage to the furnace from exposure to those gases. The second method involves the use of a controlled atmosphere, high-temperature tube furnace that would allow the fabrication of surrogate alloy ingots of up to 50 g size and with much greater control of cover gas mixing and introduction. Also a much smaller volumes of gas would be required using the tube furnace than by using the glovebox.

To perform the controlled atmosphere experiments, a 1700° C tube furnace was procured from Sentro Tech Corp. (Berea, OH) with a high-temperature ceramic tube and atmosphere control system as shown in figure 19.

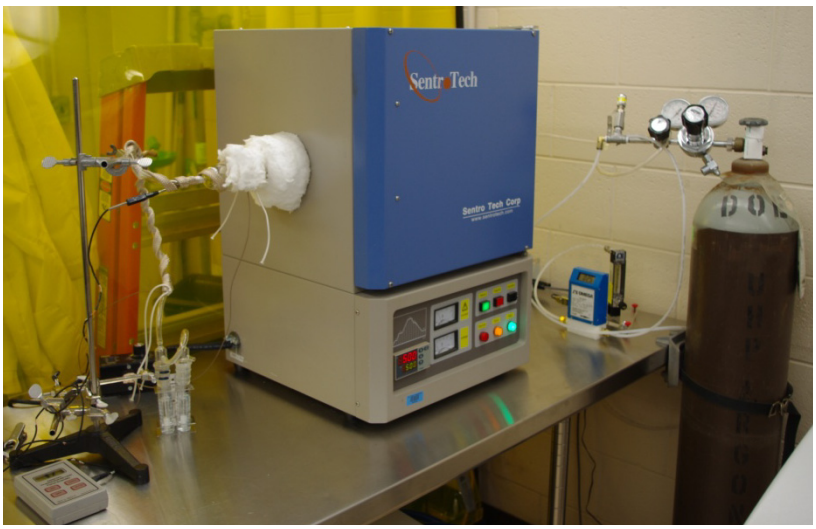

Figure 19. High-temperature (1700° C) Sentro Tech tube furnace and cover gas control system to be used for reducing atmosphere alloy fabrication.

The first phase of the reductive atmosphere experiments will be to study oxide formation during alloy fabrication by introducing differing concentrations of oxygen to the Ar cover gas, then analyzing the resulting slag layer on the alloy ingots. Slag layer formation will also be investigated by adding solid oxide impurities to the ingots followed by measurement of the slag layer. Three ingots will be produced based on the RAW-1(Re) composition described above, but at 10 to 20 g size to conserve material. Ingots will be fabricated in the presence of consecutively higher concentrations of 200, 500 and 1000 ppm oxygen in the Ar cover gas. After fabrication, the ingots will be sectioned and the surface layers analyzed by electron microscopy to measure the degree of slag layer or internal oxide phase formation. The results of slag layer formation from the first three ingots will then dictate the second phase of the experiment where an excess of hydrogen gas will be introduced to the Ar/O_2 mixture cover gas to determine the effectiveness of maintaining a reducing atmosphere on slay layer or the formation other oxide phases within the ingot.

4.2 Effect of Reductive Additives to Oxide Formation in the Alloy Waste Form

A major element of the Waste Form Characterization campaign is to investigate incorporation of various waste streams into the alloy waste forms, and of particular interest is the incorporation of the unidssolved solids (UDS) from the acidic dissolution of used oxide fuels. The range of compositions of UDS from the dissolution of oxide fuels has not been characterized and varies with fuel irradiation history and dissolution processing conditions. The alloy component of the UDS is the fission product, five-metal epsilon phase containing Mo,Tc, Ru, Rh, Pd (Te has also been observed in the ε-alloy); and it is this waste stream that is so compatible with the proposed alloy waste form. Components of the UDS that are less understood are the oxides phases. Conflicting information exist as to the oxide content of the UDS, and if the UDS does contain substantial quantities of oxide material, this may greatly complicate the fabrication and degrade the performance of the alloy waste form.

As an example to the conflicting concentration of oxide in the UDS, analysis of the CETE UDS product [8] indicates very high oxide content. This fuel was subjected to voloxidation prior to dissolution, which certainly increases the oxide content significantly. However; other investigations suggest a majority of the UDS is metallic. Analysis of UDS from the dissolution of Belgium Reactor 3 fuel, even after high-temperature voloxidation, indicates no oxide content in the UDS material [9]. Regardless, it is likely that the UDS can, under certain processing conditions, contain some amount of oxide such as zirconium oxide and/or molybdenum oxide. As mentioned above, if these oxides exist in the alloy waste form at less than approximately 1 wt%, it will probably not be detrimental to the fabrication or the performance of the waste form. If the oxide content is greater than 10 wt%, adverse affects can result during alloy fabrication, as demonstrated by L. Olson at SRNL [8] and presumably on the performance of the waste form as well.

If oxides are present in the UDS at appreciable quantities, it would be desirable to add a reductant to convert as much of the oxide as possible to the metallic state. In the case of molybdenum oxide, the SRNL study indicated the reduction of MoO_3 to Mo in the presence of Zr metal, thus Zr acts as the reductant [8]. Of course, there is no net gain by the reduction MoO_3 by Zr as a corresponding quantity of ZrO_2 is formed. A desirable goal would be to use some reducing agent to reduce the overall oxide content in the alloy. Ideal reducing agents would be H_2 or carbon so that upon reduction of the metal oxide, the reducing agent would volatize and not accumulate in the alloy melt. For the reduction of ZrO_2 , neither H_2 nor carbon are thermodynamically favorable reducing agents to convert zirconium to the metallic state (HSC Chemistry, V.5, Outokumpu Research Organization, Pori, Finland). Other metals, such as Ca, Mg, Y, the lanthanides and many actinides would be thermodynamically favorable reducing agents to ZrO_2, as shown in figure 20, but the end result would still be an equivalent amount of oxide in the alloy, just formed from a different metal.

It appears that if the UDS has appreciable quantities of ZrO_2, little could be done by way of a 'simple' chemical addition to reduce the overall oxide content of the alloy waste form. Of course, more complicated chemical methods exist, such as chlorination of ZrO_2 to volatilize the Zr, but these more complicated methods would be counterproductive to waste form production and are not considered in this study. From this analysis, two proposals are presented. The first would be to physically separate the oxide and metallic components of the UDS. The second is to optimize melt conditions so that the final melted product consists of a dense, consolidated alloy component on the bottom of the melt, and the lighter oxide component on top of the melt that could then be physically separated if required.

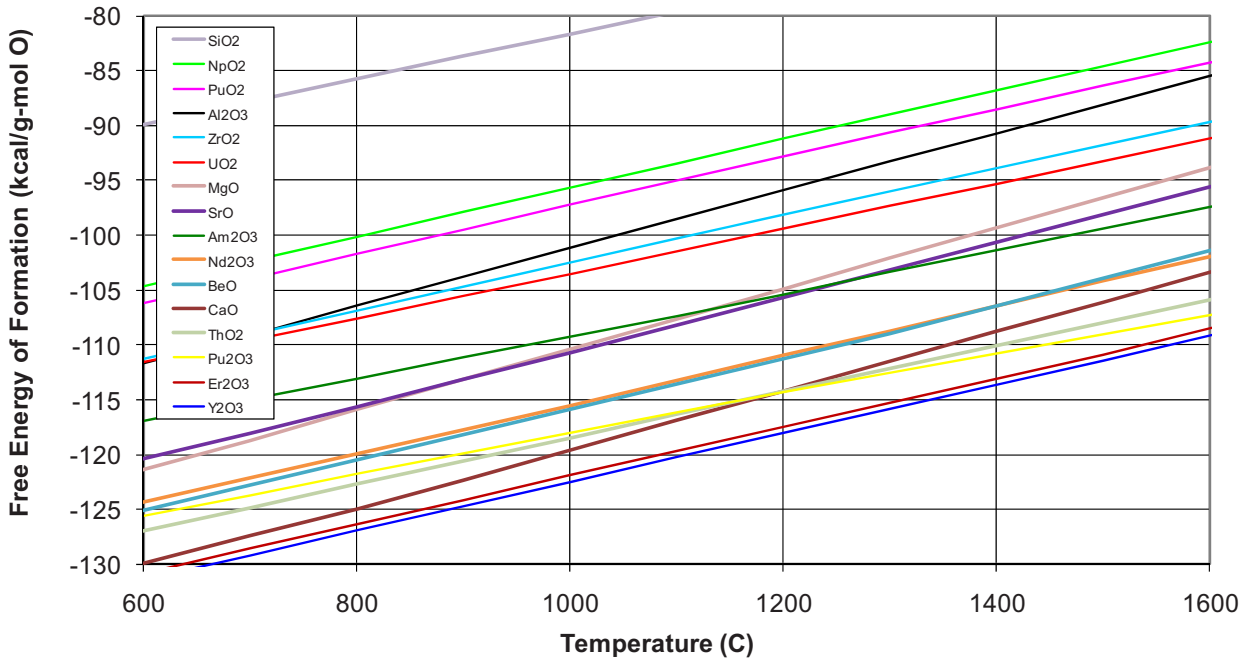

Figure 20. Free energy of formation of various metal oxides from 600° C to 1600° C indicating what metal species could reduce ZrO_2 to the metallic state (metal oxides that have more negative energies of formation).

The experimental plan for this phase of the project is to investigate melting conditions of a 50:50 metal to oxide mixture using both resistive heating and induction heating furnaces. Also to be investigated are crucible geometries that would allow easier separation of the oxide and metallic components of the melt.

5. Summary

This report describes the fabrication of two reference alloy waste forms, RAW-1(Re) and RAW-(Tc) using an optimized loading and heating method. The composition of the alloy materials was based on a generalized formulation to process various proposed feed streams resulting from the processing of used fuel. Waste elements are introduced into molten steel during alloy fabrication and, upon solidification, become incorporated into durable iron-based intermetallic phases of the alloy waste form. The first alloy ingot contained surrogate (non-radioactive), transition-metal fission products with rhenium acting as a surrogate for technetium. The second alloy ingot contained the same components as the first ingot, but included radioactive Tc-99 instead of rhenium. Understanding technetium behavior in the waste form is of particular importance due the longevity of Tc-99 and its mobility in the biosphere in the oxide form. RAW-1(Re) and RAW-1(Tc) are currently being used as test specimens in the comprehensive testing program investigating the corrosion and radionuclide release mechanisms of the representative alloy waste form.

Also described in this report is the experimental plan to study the effects of reducing atmospheres and reducing additives to the alloy material during fabrication in an attempt to maximize the oxide content of waste streams that can be accommodated in the alloy waste form. Activities described in the experimental plan will be performed in FY12. The first aspect of the experimental plan is to study oxide formation on the alloy by introducing O_2 impurities in the melt cover gas or from added oxide impurities in the feed materials. Reducing atmospheres will then be introduced to the melt cover gas in an attempt to minimize oxide formation during alloy fabrication. The second phase of the experimental plan is to investigate melting parameters associated with alloy fabrication to allow the separation of slag and alloy components of the melt.

6. References

1. S.M. Frank, D.D. Keiser, Jr, and K.C. Marsden, Immobilization of Technetium in a Metallic Waste Form, Proceedings of GLOBAL 2007, INL/CON-07-12887, Boise, ID, USA (2007).

2. W.L. Ebert, J.C. Cunnane, S.M. Frank, and M.J. Williamson, Immobilization of Tc in a Metallic Waste Form, in Materials Challenges in Alternative and Renewable Energy: Ceramic Transactions, Volume 224 (eds G. Wicks, J. Simon, R. Zidan, E. Lara-Curzio, T. Adams, J. Zayas, A. Karkamkar, R. Sindelar and B. Garcia-Diaz), John Wiley & Sons, Inc., Hoboken, NJ, USA (2010).

3. W. Ebert; Formulation of Reference Alloy Waste Form RAW-1, FCRD-WAST-2011-000004, (2011).

4. S.G. Johnson, S.M. Frank, M. Noy, T. DiSanto, and D.D. Keiser, Jr., Corrosion Characteristics of the Metallic Waste Form from the Electrometallurgical Treatment Process: Technetium and Uranium Behavior During Long-Term Immersion Test, Radioactive Waste Management and Env. Res,. 22, 300-326 (2002).

5. J. Fortner, Personal communication April 26, 2011, presentation at Alloy Waste Form videoconference workshop.

6. K.C. Marsden, S.M. Frank, and B.R. Westphal, The Metallic Waste Form from Electrometallurgical Treatment of EBR-II Spent Fuel: From Development to Full-Scale Production," Integrated Radioactive Waste Management in Future Fuel Cycles, Charleston, South Carolina, November (2009).

7. S.M. McDeavitt and D.P. Abraham, Investigation of Slags, Metal Waste Form Handbook, ed. D.P. Abraham, Argonne National Laboratory Report: ANL-NT-121, Argonne, IL (1999).

8. L. Olson, FY11, Status Report: Oxide Incorporation in Iron Based Alloy Waste Forms, FCRD-SWR-2011-000222 (2011).

9. B.R. Westphal and T.P. O'Holleran, Personal communication April 26, 2011, presentation at Alloy Waste Form videoconference workshop.